Galactic Isotopic Decomposition for the Sculptor Dwarf Spheroidal Galaxy

Kanishk Pandey | Christopher West
Carleton College, Northfield, MN, 55057

Purpose:

Stellar models and galactic chemical evolution (GCE) models require an initial isotopic abundance set to properly simulate stars and galaxies. When modelling the sun, the solar abundance pattern is used as an initial isotopic abundance set. However, when modelling environments outside our solar neighborhood, the solar abundance pattern may not be a good representation of the environment. Therefore, it is difficult to devise an accurate GCE model for galaxies other than the Milky Way, such as neighboring dwarf spheroidal (dSph) galaxies. More accurate models can provide a better understanding of the chemical evolution differences between dSph galaxies and spiral galaxies like the Milky Way.

We present an isotopic history for the Sculptor dwarf spheroidal (dSph) galaxy based on the astrophysical processes responsible for isotopic production, which is a complementary approach to GCE models. The procedure is similar to the approach outlined by West & Heger (2013) who modelled the Milky Way. The result is a complete isotopic history for the processes considered of the Sculptor dSph from BBN to the present, which can be compared with the isotopic history of the MW.

Astrophysical Processes:

Isotopic abundances are governed by numerous astrophysical processes.

Astrophysical Process	Salient Elements Produced
Big Bang Nucleosynthesis (BBN)	H, He, Li
Massive Stars	Most α-elements between He to iron peak (eg. O, Mg, Si, Ca, Ti)
Type 1a Supernovae	Most iron peak elements (eg. Fe, Ni, Co, Mn, Cr)
Neutron Capture (s- and r-) Processes	Almost all elements after iron (eg. Sr, Ba, Eu, Pb)

Previous chemical evolution models for dSphs suggest the following general trends:

- dSphs are more dominated by contributions from Type1a SNe and AGB stars than the Milky Way
- The Type1a onset occurs earlier in dSphs than the Milky Way
- The slope of the Type1a onset is steeper in dSphs than in the Milky Way
- The r-process to s-process transition occurs earlier for dSphs than for the Milky Way

Methodology:

We used the procedure outlined by West & Heger (2013) to model the isotopic history of the Sculptor dSph galaxy. Three states were chosen as fixed points for the model: BBN (initial), [Fe/H] = -3 (intermediate), and late stage (final). Parametric equations were determined for each astrophysical process. In each parametric equation, the dimensionless model parameter "ξ" is monotonic with metallicity and time. At ξ = 0, the galaxy is in BBN composition and at ξ = 1, the galaxy is in its current state. Best-fit free parameter values were found by fitting elemental abundances to observed Sculptor data.

Sculptor's Low Z Evolution

At the intermediate state of the model ([Fe/H] = -3), massive star and Type1a yields were scaled to fix a third point in Sculptor's evolution. This point was used to calculate the slope in the massive star functional form.

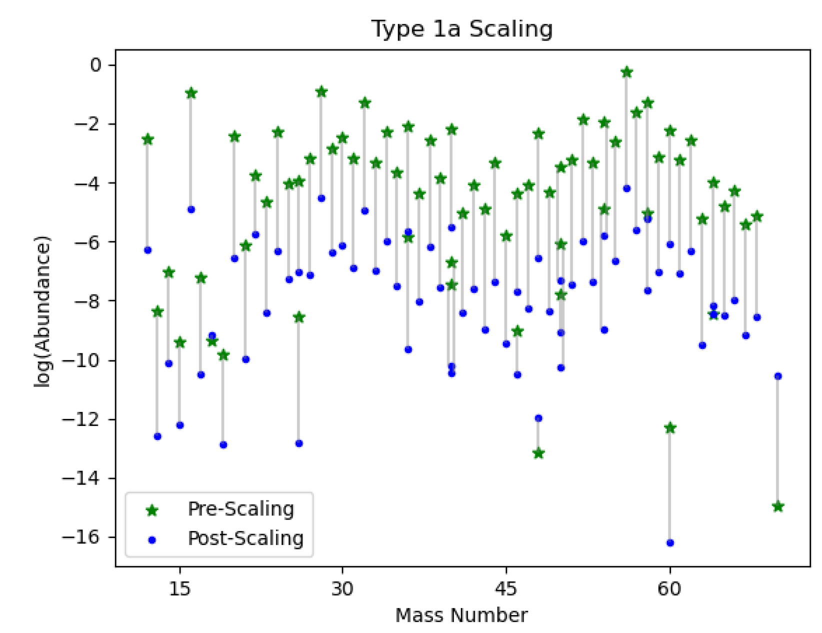

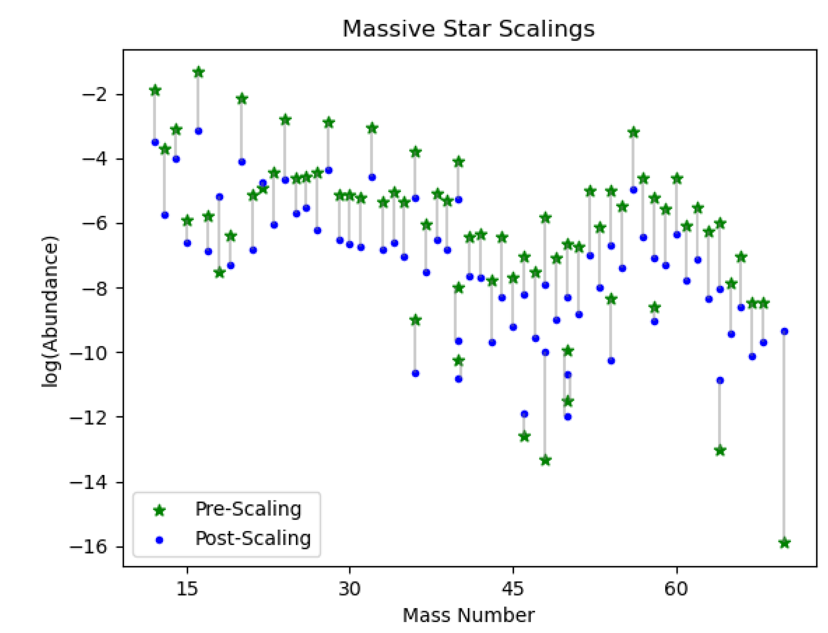

Sculptor's High Z Evolution

The final state of the model was derived by running the OMEGA GCE and extracting isotopic yields at the late stage of Sculptor's evolution ([Fe/H] = -1.25).

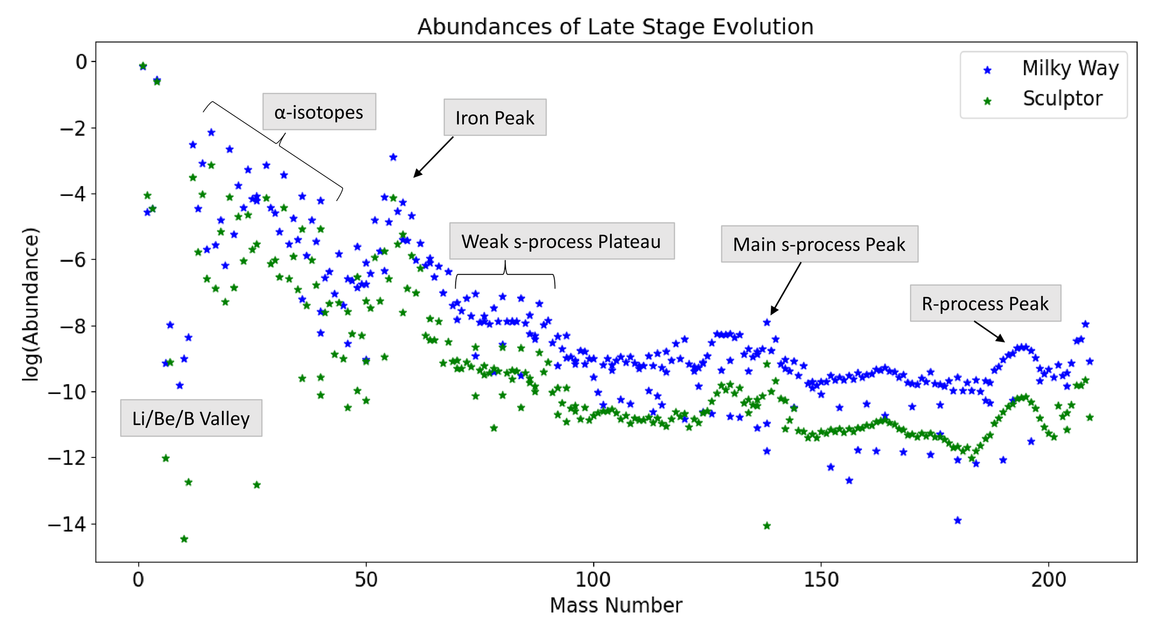

The Model:

Motivation for Functional Forms:

$$\text{Primary Processes: } \frac{\partial X_{i,p}}{\partial Z} = \text{const.} \rightarrow X_{i,p} \propto Z$$

$$\text{Secondary Processes: } \frac{\partial X_{i,s}}{\partial Z} = X_{j,p} \rightarrow X_{i,s} \propto Z^2$$

These relations motivate the functional forms for different astrophysical processes.

Example of Fe Functional Form:

$$^{56}Fe(\xi) = {}^{56}Fe^{1a}_{\odot} \cdot \xi \cdot \frac{[tanh(a\cdot\xi-b)+tanh(b)]}{[tanh(a-b)+tanh(b)]} + 10^{m_{Fe_{56}}(log(\xi)-log(\xi_{low}))+log\left(x_i^{sim}\right)}$$

- Solar abundance from Type1a SNe
- Contribution from Type1a SNe
- Solar abundance from Massive Stars (contained in slope)
- Contribution from Massive Stars

Similar equations are found for ^{54}Fe, ^{57}Fe, and ^{58}Fe. The isotopic abundances are then summed into elemental abundances.

$$Fe(\xi) = {}^{54}Fe(\xi) + {}^{56}Fe(\xi) + {}^{57}Fe(\xi) + {}^{58}Fe(\xi)$$

Astrophysical Process	Functional Form
Massive Stars	$log\left(X_i^*(\xi)\right) = m_i\left(log(\xi) - log(\xi_{low})\right) + log\left(X_i^{sim}\right)$, where $m_i \equiv \frac{log\left(X_{i,f}^{massive}\right) - log\left(X_i^{sim}\right)}{log(\xi_\odot) - log(\xi_{low})}$
Type 1a Supernovae	$X_i^{Ia}(\xi) = X_{i,\odot}^{Ia} \cdot \xi \cdot \frac{[tanh(a\cdot\xi - b) + tanh(b)]}{[tanh(a-b) + tanh(b)]}$
S-process	$X_i^{hs}(\xi) = X_{i,\odot}^{hs} \cdot \xi^h$
R-process	$X_i^r(\xi) = X_{i,\odot}^r \cdot \xi^p$

Parameters	Sculptor Best-fit Value	Milky Way Best-fit Value	Description
a	3.903	5.024	Type 1a tanh scaling factor
b	-0.192	2.722	Type 1a tanh shifting factor
f	0.851	0.693	Fraction of solar ^{56}Fe from Type 1a
h	1.05	1.509	s-process exponent

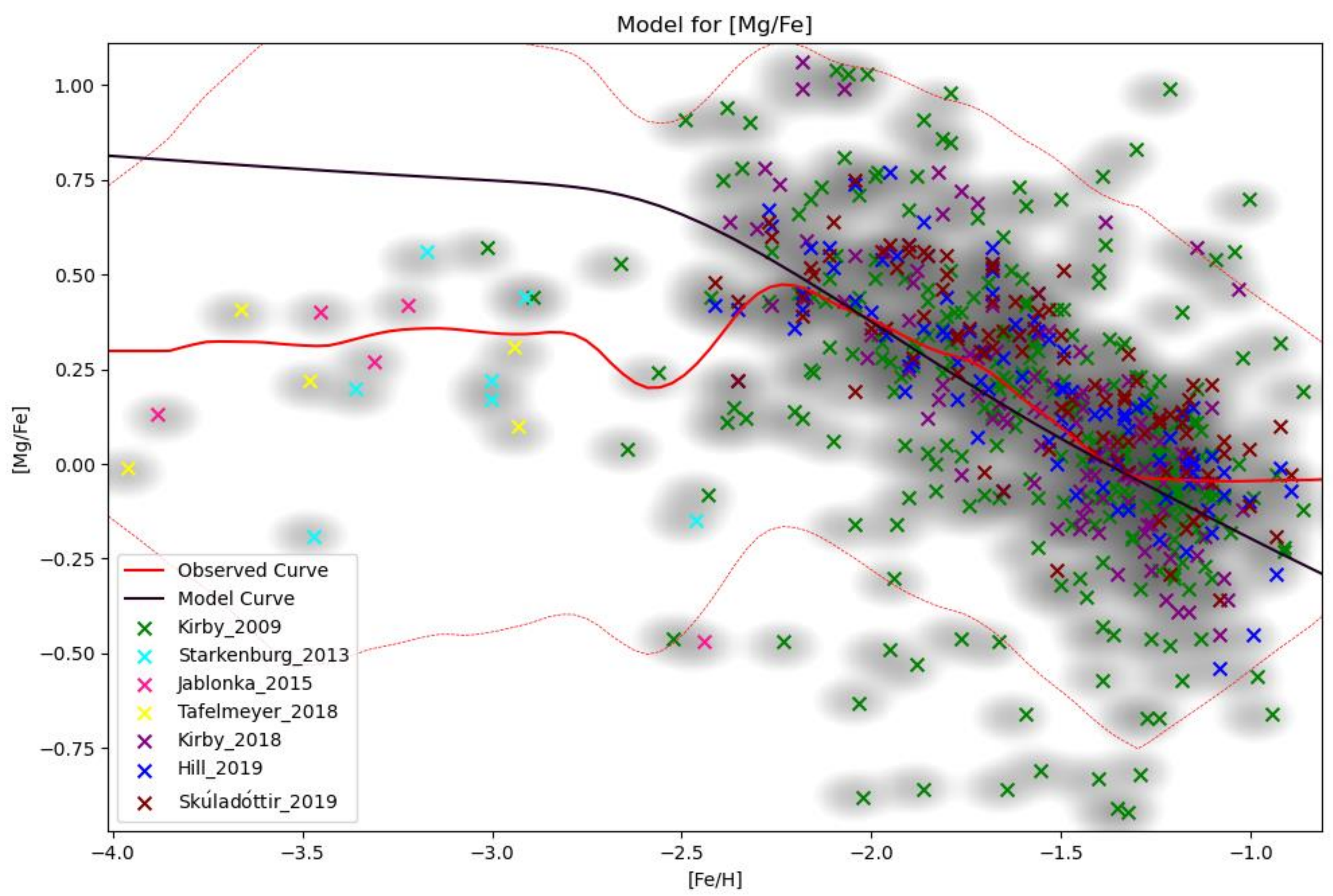

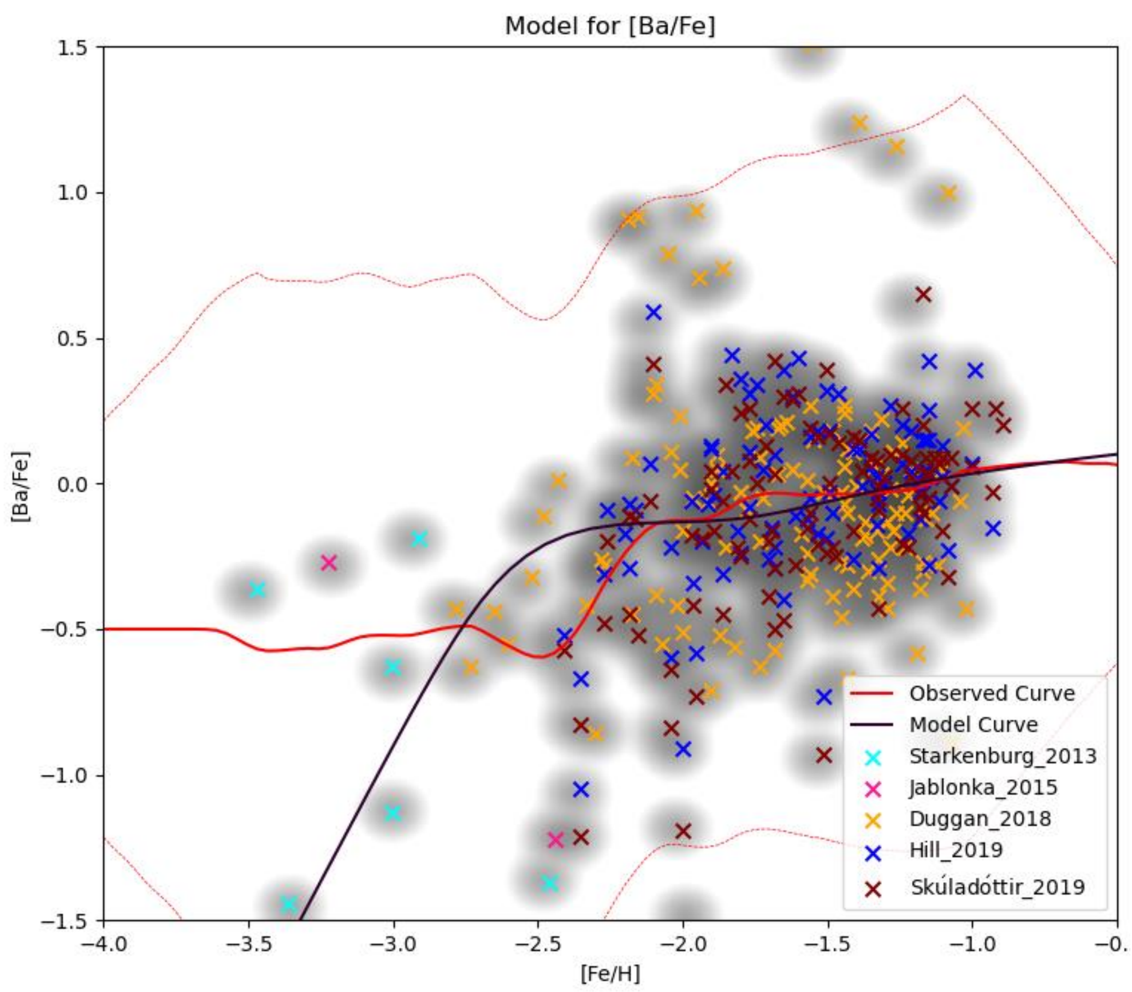

Conclusions:

- Type 1a SNe contribute ≈85% of solar ^{56}Fe in Sculptor, which is greater than the Type 1a SNe contribution in the Milky Way (≈70%)
- The Type1a onset occurs earlier in dSph galaxies than the Milky Way
- The Type1a onset in Sculptor begins at [Fe/H] = -1.43, which is near predictions from previous dSph galaxy studies (-2.0 ≤ [Fe/H] ≤ -1.6)
- The impact of Type1a SNe in Sculptor occurred over a shorter time interval than in the Milky Way
- The s-process had a primary dependence during the late stage of Sculptor's evolution

Future Directions:

- Continue fitting Ba to find the best-fit free parameter value for h
- Fit Eu and find best-fit free parameter value for p
- Possibly separate weak and main s-process scalings
- Identify a Ni/Na correlation suggested by previous studies and compare it to the Milky Way

Acknowledgements:

Thank you to my advisor, Chris, for guiding me throughout this journey and for inspiring me to become a researcher. Thanks to Carleton College for promoting undergraduate research and providing a platform for students to share their research experiences.

References:

West, C., & Heger, A. 2013, ApJ, 774, 24, doi: 10.1088/0004-637X/774/1/75
Leung, S.-C., & Nomoto, K. 2020, ApJ, 888, 44, doi: 10.3847/1538-4357/ab5c1f
Lanfranchi, G. A., & Matteucci, F. 2003, MNRAS, 345, 71, doi: 10.1046/j.1365-8711.2003.06919.x
Kirby, E. N., Guhathakurta, P., Bolte, M., Sneden, C., & Geha, M. C. 2009, ApJ, 705, 328, doi: 10.1088/0004-637X/705/1/328
Heger, A., & Woosley, S. E. 2010, ApJ, 724, 341, doi: 10.1088/0004-637X/724/1/341
Tolstoy, E., Hill, V., & Tosi, M. 2009, ARA&A, 47, 371, doi: 10.1146/annurev-astro-082708-101650
Kirby, E. N., Xie, J. L., Guo, R., et al. 2019, ApJ, 881, 16, doi: 10.3847/1538-4357/ab2c02
OMEGA GCE: (https://github.com/NuGrid/NuPyCEE/blob/bfdadceb8880ef37506c278f8de5e6c616cf8962/omega.py)